Identification of monoclonal antibody binding domains of Na^+,K^+-ATPase by immunoelectron microscopy

H. Ping Ting-Beall[1], Harry C. Beall[1], David F. Hastings[1,*], Mark L. Friedman[2,**] and William J. Ball, Jr.[2]

[1]*Department of Cell Biology, Duke University Medical Center, Durham, NC 27710* and [2]*Department of Pharmacology and Cell Biophysics, University of Cincinnati College of Medicine, Cincinnati, OH 45267, USA*

Received 10 April 1990

Treatment of purified preparations of porcine Na^+,K^+-ATPase with phospholipase A_2, $MgCl_2$ and $NaVO_3$ leads to the formation of two-dimensional crystals exclusively in a dimeric configuration. Two-dimensional computer-averaged projections of the electron microscopy images of the crystalline enzyme with bound F_{ab} fragments of monoclonal antibody M10-P5-C11 were accomplished using image enhancement software and showed that the antibody fragments caused only a modest increase in the unit cell size, while reducing the extent of asymmetry of the two promoters in each unit cell. The digital imaging also showed that the antibody's epitope on the α subunit resides on the 'lobe' or 'hook' region of the intracellular portion of the enzyme. Since functional studies indicate that M10-P5-C11 binds near or between the ATP binding site and the phosphorylation site, this visualized 'lobe' region of α may comprise the catalytic site. In addition, the binding of another inhibitory antibody, 9-A5, has been found to prevent crystal formation and the presence of the carbohydrate sugars on the enzyme's β subunit shown to be required for crystal formation.

Na^+,K^+-ATPase; Monoclonal antibody; Image processing; Immunoelectron microscopy

1. INTRODUCTION

The membrane-bound Na^+,K^+-ATPase directly couples the hydrolysis of ATP to the active transport of 3 Na^+ out of the cell and 2 K^+ into the cell and serves as the receptor for the cardiac glycosides. This enzyme has been isolated, purified and characterized from numerous diverse sources [1]. Considerable data concerning the kinetics and partial reactions of the enzyme [1–3] and the amino acid sequences of both the α and β subunits from various tissues is now known [4–7]; however, the ligand binding sites on α have not been identified nor is the actual molecular mechanism of active transport as yet understood. A significant reason for this lack of understanding of ion transport is the paucity of detailed information about the spatial relationships between the enzyme's transmembrane segments, extramembrane domains, and α and β subunits.

Final determination of Na^+,K^+-ATPase structure will require X-ray crystallographic analysis; however, the discovery of procedures to achieve two-dimensional crystalline enzyme arrays has made it possible to achieve initial electron microscopy and computer-enhanced 2-dimensional and 3-dimensional image processing studies [8–10]. Crystallization appears to be best achieved using Mg^{2+} and vanadate or phosphate conditions which stabilize E_2 conformational forms of the enzyme and results in both $\alpha\beta$ protomer and $(\alpha\beta)_2$ dimer arrays in the unit cell. However, the removal of phospholipids by phospholipase A_2 also results in the formation of $(\alpha\beta)_2$ dimeric sheets [11]. In general, imaging procedures have shown that the detectable extramembranous mass appears to consist of the cytoplasmic exposed region of the enzyme which is seen as a massive 'body' and a thin 'lobe' or 'hook' that orientates the molecules in a diagonal manner.

Since no specific functional identification of these exposed regions of the crystallized enzyme has been achieved, we have used unique, site-directed monoclonal antibodies as probes of the enzyme. In the work presented here we have utilized two well-characterized monoclonal antibodies: M10-P5-C11 [12] and 9-A5 [13]. Both of these antibodies are directed against intracellular regions of the α subunit of the holoenzyme and inhibit ATPase function. Antibody 9-A5 binding has been localized to a peptide region which includes both the phosphorylation site and the cardiac glycoside labeling segment of α [14]. In the presence of Mg^{2+}, 9-A5 stabilizes an E_1Mg^{2+} conformation of Na^+,K^+-ATPase thereby inhibiting both the Na^+,K^+-dependent ATPase and K^+-dependent *p*-nitrophenylphosphatase activities [15]. Antibody M10-P5-C11 binds at a site distinct, but proximal to both the ATP and phosphorylation site. It inhibits the ATPase activity and $E_1 \sim P$ intermediate formation without significant effects on

Correspondence address: W.J. Ball Jr., Department of Mechanical Engineering and Materials Science, School of Engineering, Duke University, Durham, NC 27706, USA

* *Present address:* Micro Systems Engineering Inc., 6024 S.W. Jean Road, B-4, Lake Oswego, OR 97035, USA

** *Present address:* Miles Inc., P.O. Box 70, Elkhart, IN 46515, USA.

Published by Elsevier Science Publishers B.V. (Biomedical Division)
00145793/90/$3.50

pNPPase activity, E_2-P dephosphorylation, or $E_1Na \rightleftarrows E_2K$ transitions [12,15].

Utilizing electron microscopy and digital image processing computer programs [16], we have generated 2-dimensional image projections of Na^+,K^+-ATPase with bound antibody M10-P5-C11. These data show that the 'lobe' region of $\alpha\beta$ monomers contains the antibody epitope, and therefore it consists of a visualized region of α that may comprise the enzyme's ATP binding and phosphorylation sites. In addition we have found that antibody 9-A5 binding occurs at a spatially distinct site of α which prevents crystal formation, and that the carbohydrate moieties of β contribute to dimeric crystal formation.

2. MATERIALS AND METHODS

Membrane-bound Na^+,K^+-ATPase was isolated and purified from outer medulla of fresh pig kidney as described previously by Jørgensen [17], Freytag and Reynolds [18], and Hastings et al. [19]. The deglycosylation of Na^+,K^+-ATPase was carried out at 37°C in a buffer containing 0.1 M sodium phosphate, 5 mM EDTA, 1% mercaptoethanol, 0.005% sodium dodecylsulfate and 0.0125% NP-40, pH 7.15. Na^+,K^+-ATPase (0.5 mg/ml) was incubated in this buffer 4 h with a 1/200 w/w ratio of neuraminidase, then an additional 18 h upon addition of endoglycosidase F (8 U EndoF/mg Na^+,K^+-ATPase). The reaction mixture was centrifuged for 1 h at 100,000 × g, the pelleted Na^+,K^+-ATPase resuspended in a 50 mM Tris, 1 mM EGTA, pH 7.2 solution and then centrifuged and resuspended a second time before being prepared for crystallization. Monoclonal antibodies M10-P5-C11 and 9-A5 were affinity-purified from the ascites fluid of mice inoculated with the cloned hybridoma cell lines using protein A-Sepharose chromatography [20]. F_{ab} fragments were obtained by digestion of the mouse IgG_1 with papain [21] and elution from a protein A-Sepharose column at pH 8.

Before induction of enzyme crystallization, the purified pig kidney Na^+,K^+-ATPase was suspended in 10 mM Tris-HCl (pH 7.5) at 10 μg/ml with various concentrations of the intact immunoglobulins or their F_{ab} fragments for 1 h at 20°C. The crystallization procedures were similar to those reported by Mohraz et al. [11]. Briefly, 10 μg/ml of enzyme was incubated in the buffer, with 4 units/ml of bee venom phospholipase A_2 (Sigma), 1 mM $CaCl_2$, 5 mM $MgCl_2$ and 1 mM $NaVO_3$ for 2 h at 20°C with approximately 90% of membrane fragments showing crystalline assays. After crystallization, the mem-

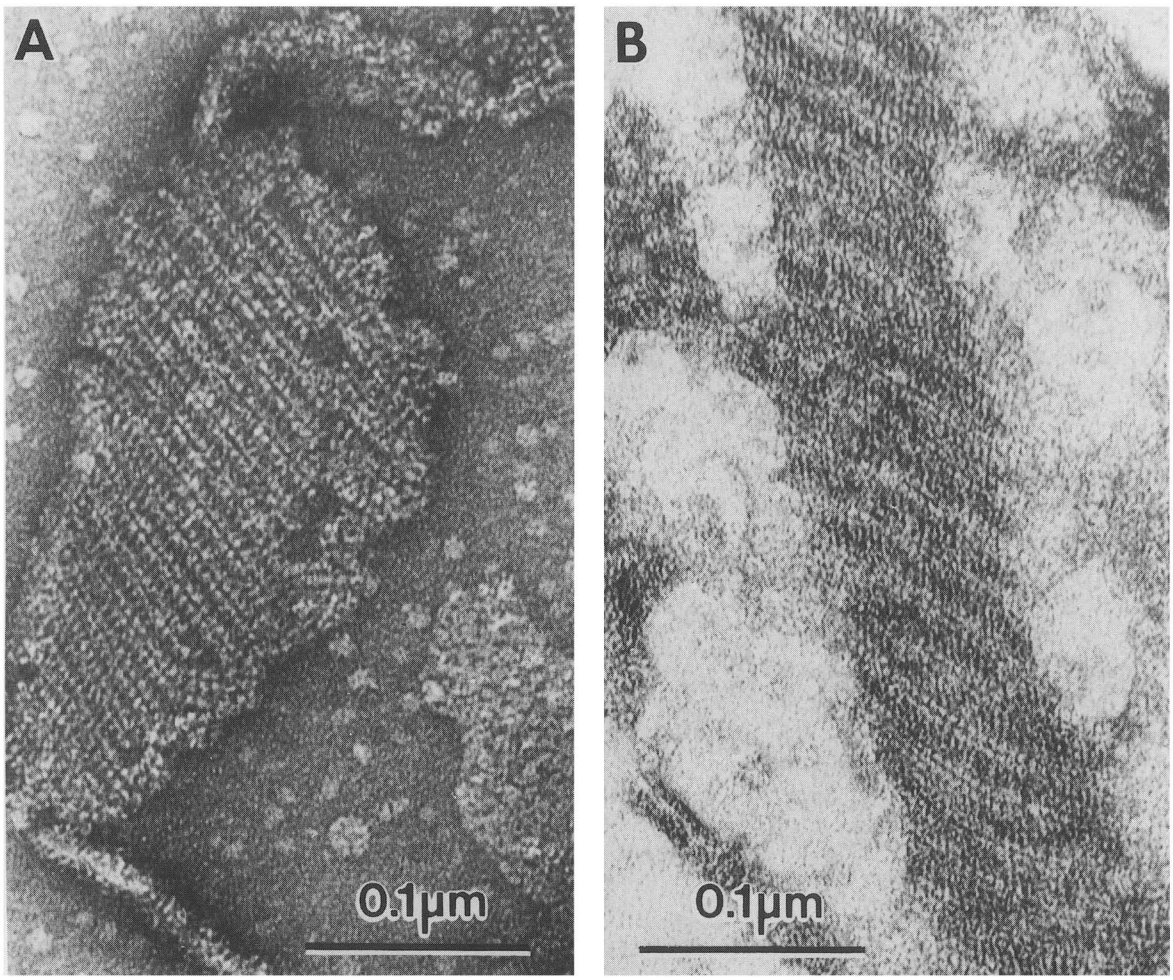

Fig. 1. (A) Phospholipase A_2 induced crystalline arrays of purified Na^+,K^+-ATPase stained with 2% unbuffered uranyl acetate. 10 μg/ml of enzyme was incubated in a buffer solution containing 4 units/ml of phospholipase A_2, 1 mM $CaCl_2$ and 1 mM $NaVO_3$ for 2 h at 20°C. (B) Phospholipase A_2 induced crystalline arrays of purified Na^+,K^+-ATPase with bound antibody M10-P5-C11. Before crystallization, 10 μg/ml of antibody M10-P5-C11 was incubated with 5 μg/ml of 10 mM Tris-HCl (pH 7.5) for 1 h at 20°C, and the crystallization conditions were the same as described in (A) and section 2.

brane fragments were adsorbed onto freshly glow-discharged, carbon-coated grids and stained with 2% unbuffered uranyl acetate. Stained specimens were examined and imaged in a Philips 301 electron microscope utilizing a 20 μm objective aperture. The micrograph films were scanned on a Perkin-Elmer PDS Model 1010A flatbed microdensitometer. Two-dimensional averaged projections of the crystals were calculated by the technique of correlation averaging, utilizing SPIDER (System for Processing of Image Data in Electron microscopy and Related fields) image processing software obtained from the New York State Department of Health at Albany, NY [22,23]. This program, with recent modifications, has been described in detail and projection images of Ca^{2+}-ATPase crystals generated by this correlation averaging procedure have been compared and matched [16] to those previously published by Taylor et al. [24] using Fourier transforms.

3. RESULTS AND DISCUSSION

In the presence of phospholipase A_2, Mg^{2+} and vanadate the purified pig kidney Na^+,K^+-ATPase molecules formed oval patches of two-dimensional crystals approximately 800×200 nm (Fig. 1A). The crystal arrays were exclusively in the dimeric form with an $(\alpha\beta)_2$ structure in the unit cells (Fig. 3A) and the dimers formed ribbons of paired molecules similar to those seen by Mohraz et al. [11,25]. The central portion of the ribbons contained narrow, intense stain grooves, and another set of wider, less intense stain grooves ran between ribbons and parallel to the intense stain grooves. The bodies of the unit cell formed a parallelogram, 13.3×4.59 nm with the obtuse angle γ equal to 98°; values comparable to those obtained by others [8,10,11].

Since neither of the monoclonal antibodies was originally raised to this enzyme preparation, their ability to bind to the pig enzyme was determined. Solution phase binding, or competition, studies similar to those performed previously with antibody 9-A5 [15] but using the porcine enzyme preparation showed that, at approximately stoichiometric ratios of antibody to enzyme, about 50% of the antibody was bound and that, for both antibodies, binding was saturated using a 2–3-fold excess of enzyme. Enzyme concentration versus percent antibody bound curves further showed that M10-P5-C11 has similar affinities for both the pig and lamb enzymes, while 9-A5 actually had a somewhat higher affinity towards the pig enzyme. As with the

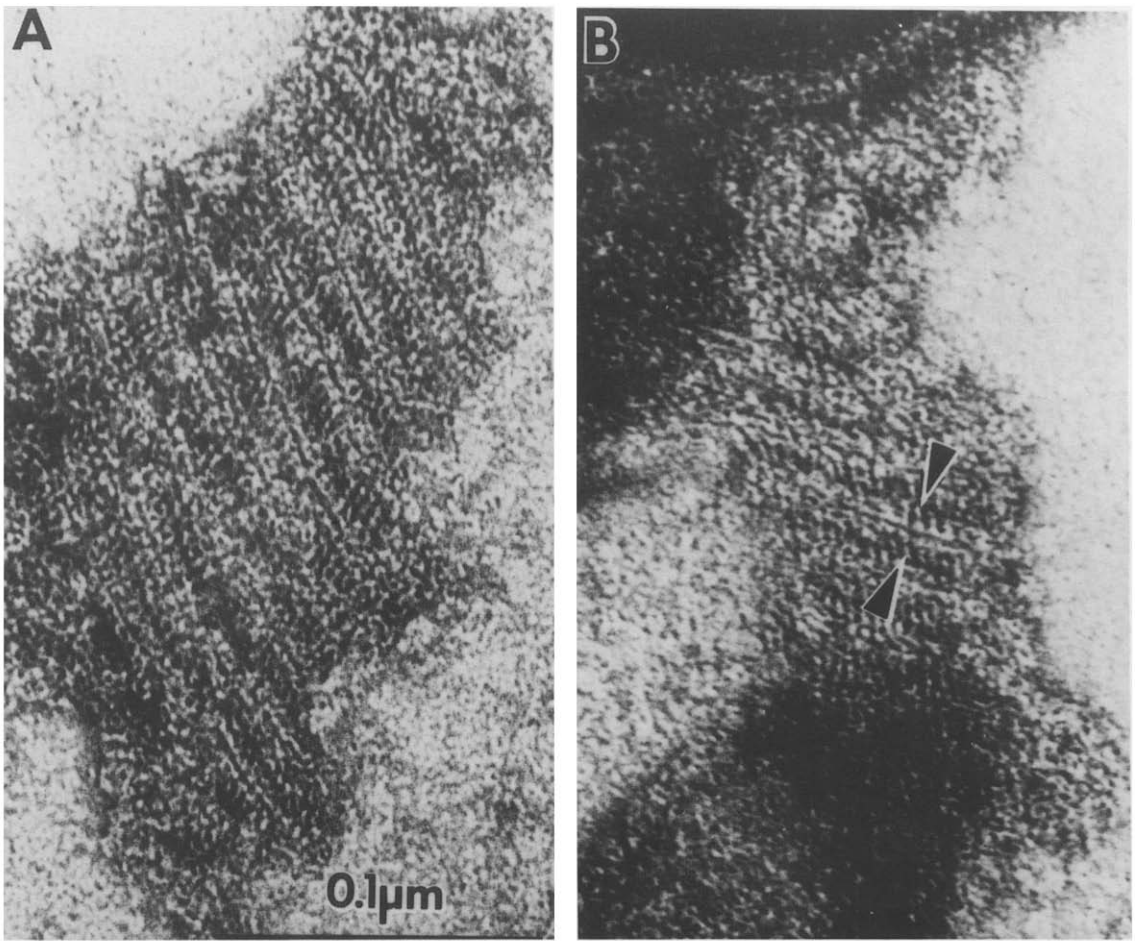

Fig. 2. Phospholipase A_2 induced Na^+,K^+-ATPase crystalline arrays with bound F_{ab} fragments of M10-P5-C11. 20 μg/ml of F_{ab} fragments were incubated with 10 μg/ml of Na^+,K^+-ATPase for 1 h at 20°C. The crystallization conditions were the same as in Fig. 1.

lamb kidney enzyme both antibodies bound preferentially to native rather than denatured porcine enzyme.

In the presence of antibody M10-P5-C11, the Na^+, K^+-ATPase was found to crystallize into ribbons of dimers (Fig. 1B). However, the repeat periods between the intense stain grooves increased from 140 Å to 186 Å, a 33% increase and the less stained grooves between the ribbons were no longer visible (Fig. 1B). Because of this distortion in the crystalline arrays and the loss of image resolution caused by the bound, but flexible, immunoglobulin, we were unable to further image process the micrographs. In contrast, when antibody 9-A5 bound to the enzyme there was no crystallization.

Because of the crystal distortions observed using intact M10-P5-C11 antibody, F_{ab} fragments were generated and bound to the enzyme. In these experiments, two-dimensional crystals were observed within 2 h of beginning the crystallization process. When the F_{ab} fragment:enzyme ratio (w/w) was 2:1 or greater (i.e. ~6:1 molar ratio), the lattice dimensions of the dimeric crystals were found to be uniformly 20% larger than the controls. Close examination of the magnified micrographs (Fig. 2A, B) revealed the shape and density of the head region or 'body' of the visualized molecules to be unchanged. However, additional mass appeared at the smaller end of the 'lobe' or 'hook' (see arrowheads on Fig. 2B) of the enzyme. This mass and the reorientation of protomers on the right border of the dimer ribbons can be clearly seen by a direct comparison of the two reconstructed images; the control image of Fig. 3A and the image with bound M10-P5-C11 F_{ab} (Fig. 3B). The dimensions of the unit cells were also altered to 16.0×5.1 nm with $\gamma = 98°$. It had originally been suggested by Mohraz et al. [9] that the 'hook' region of the $\alpha\beta$ protomers represented the visualization of the β-subunit. This conclusion rested largely upon the fact that Castellani and Hardwicke [26] found the hook missing in the filtered image generated by crystals of the Ca^{2+}-ATPase of scallop, and this enzyme is presumed not to have an analogous β subunit. Currently this lack of a hook region is doubtful since other investigators have found the rabbit skeletal Ca^{2+}-ATPase enzyme structure to be more complex than originally thought [24,27,28]. Also, later work of Castillani et al. [29], using more detailed low dose EM imaging, has shown a complex asymmetrical shape for scallop Ca^{2+}-ATPase with the presence of a hook region similar to that of Na^+, K^+-ATPase. Consequently, Mohraz et al. [25] have modified their original proposal to suggest that the 'hook', or 'lobe', consists largely of α and that a visualized connecting 'arm' close to the membrane that links ribbons of $(\alpha\beta)$ pairs consists of β-β NH_2 terminal domain connections.

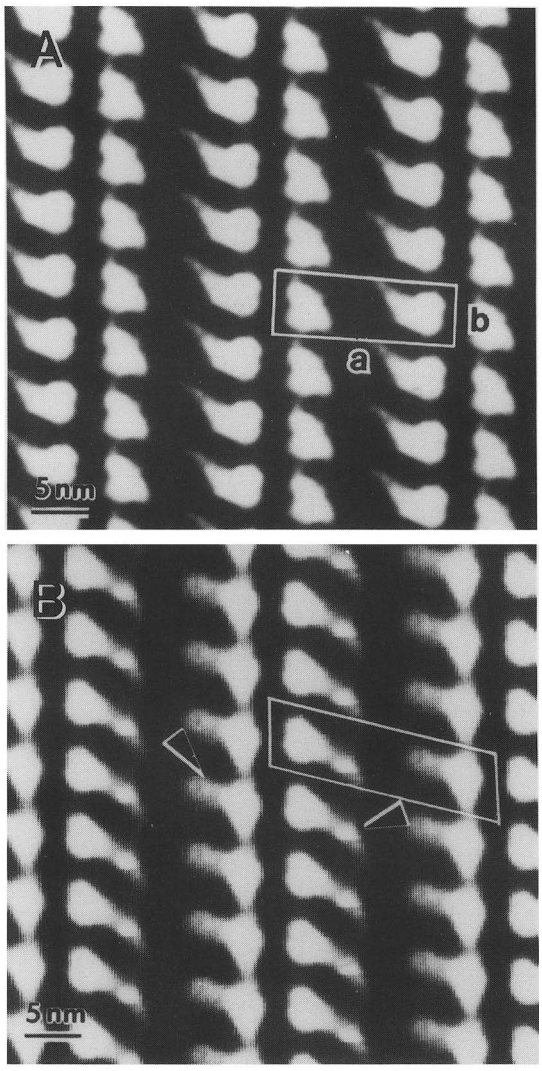

Fig. 3. Averaged images, calculated by the correlation averaging technique. (A) Control crystalline array, shown in Fig. 1A; and (B) crystalline array with bound F_{ab} fragments of M10-P5-C11, shown in Fig. 2A.

Since M10-P5-C11 binds only to α, we can conclude that this region consists primarily of α or possibly both α and β. The ability of the enzyme-F_{ab} complex to crystallize is consistent with our kinetic [12] and fluorescence spectroscopy studies [15] which suggest that M10-P5-C11 binds in a manner that does not interfere directly with ligand binding and most regulatory ligand interactions. Further since mechanistically M10-P5-C11 appears to bind close to both the ATP binding site and the phosphorylation site, the visualized lobe region may very well comprise these sites. The bound F_{ab} fragments also appear to reduce the extent of the asymmetry observed for the unit cell monomers. They may modify the monomer orientations or simply add additional mass to the lobe ends of the molecules.

Additional crystallization studies showed that 9-A5 F_{ab} fragments also prevented crystal formation. Since crystallization is facilitated by the enzyme's being in an E_2 conformation, these results suggested that 9-A5 stabilization of the $E_1 \cdot Mg^{2+}$ conformation prevented

crystal formation. However, by monitoring fluorescence intensity decreases of the FITC-labeled porcine enzyme, we found that 9-A5 binding substantially reduced the rate of the vanadate (1 mM) induced $E_1 \cdot Mg^{2+} \rightarrow E_2\text{-}VO_3Mg^{2+}$ transition but not the extent of the change. Under crystallization conditions (Mg^{2+}, Ca^{2+} and VO_3^-) 9-A5 apparently does not 'freeze' this enzyme in an $E_1 \cdot Mg^{2+}$ conformation.

Therefore, how 9-A5 binding prevents crystallization remains to be determined. 9-A5 has been shown to bind to a region adjacent (towards the CO_2-terminal end) to the trypsin cleavage site, Ile-263 that is involved in the $E_1 \rightleftarrows E_2$ transition [14,30]. This epitope, with antibody bound, may induce conformational alterations in the NH_2-terminal region of α, effecting α–α bridgings, that have been proposed to be essential for monomer ribbon formation [25] but it seems more likely that the antibody causes critical steric effects that block crystal formation.

In contrast to the intracellular surface of the enzyme, the extracellular surface of the membrane shows little structure. It is not clear why, while only a small proportion of α is thought to protrude through the membrane bilayer, β appears to have only one transmembrane segment and 80% of its sequence (AA residues, 61–302) is thought to be exposed extracellularly. It may be that the 3 sugar chains of β mask the exposed protein components. We find that the carbohydrate chains may also be essential for protomer and dimer stacking since treatment of the enzyme with neuraminidase and endoF prevent enzyme crystallation. This treatment reduces enzyme ATPase activity only moderately (< 10%) while removing a substantial portion of the sugar moieties leaving a core β_c protein and intermediary glycosylated β', and β'' forms. Thus, it appears that both protein–protein and carbohydrate-protein linked interactions are crucial to crystal formation.

Clearly the ultimate goal of 2-D and 3-D reconstructions of the Na^+, K^+-ATPase is to define its structure to the degree that specific structural features essential for ligand binding and ion transport can be identified. In these studies, we have extended our previous efforts analyzing the two-dimensional crystals of negatively stained and frozen hydrated enzyme [16,31]. While the resultant data are limited due to the paucity of monoclonal antibodies which effect N^+, K^+-ATPase function or whose sites of binding are known, the continued correlation of the 3-D localization of antibody epitopes with determinations of the in primary sequences and mechanistic involvement in enzyme function will enhance our understanding of the molecular mechanism of Na^+, K^+-ATPase action.

Acknowledgements: This work was supported by grants from the National Institute of Health: RO1-GM-27804 (H.P.T.-B), T32-HL-07382 (M.L.F.), and RO1-HL-32214 (W.J.B.). W.J.B. is an Established Investigator of the American Heart Association.

REFERENCES

[1] Jørgensen, P.L. (1982) Biochim. Biophys. Acta 694, 27–68.
[2] Glynn, I.M. (1985) in: The Enzymes of Biological Membranes, vol. 3 (Martonosi, A.N., ed) Plenum Press, New York, pp.35–114.
[3] Repke, K.R.H. (1986) Biochim. Biophys. Acta 864, 195–212.
[4] Shull, G.E., Schwartz, A. and Lingrel, J.B. (1985) Nature 316, 691–695.
[5] Shull, G.E., Lane, L.K. and Lingrel, J.B. (1986) Nature 321, 691–695.
[6] Kawakami, K., Noguchi, S., Noda, M. Takahashi, H., Ohta, T., Kawamura, M., Nojima, H., Nagano, K., Hirose, T., Inayama, S., Hayashida, H., Miyata, T. and Numa, S. (1985) Nature 316, 733–736.
[7] Noguchi, S., Noda, M., Takahashi, H., Kawakami, K., Ohta, T., Nagano, K., Hirose, T., Inayama, S., Kawamura, M. and Numa, S. (1986) FEBS Lett. 196, 315–320.
[8] Skriver, E., Maunsbach, A.B. and Jørgensen, P.L. (1981) FEBS Lett. 133, 219–222.
[9] Mohraz, M. and Smith, P.R. (1984) J. Cell Biol. 98, 1836–1841.
[10] Zampighi, G., Kyte, J. and Freytag, W. (1984) J. Cell Biol. 98, 1851–1864.
[11] Mohraz, M., Yee, M. and Smith, P.R. (1985) Ultrastructure Res. 93, 17–26.
[12] Ball, W.J. (1986) Biochemistry 25, 7155–7162.
[13] Schenk, D.B. and Leffert, H.L. (1983) Proc. Natl. Acad. Sci. USA 80, 5281–5295.
[14] Farley, R.A., Ochoa, G.T. and Kudrow, A. (1986) Am. J. Physiol. 250, C896–C906.
[15] Friedman, M.L. and Ball, W.J. (1989) Biochim. Biophys. Acta 995, 42–53.
[16] Beall, H.C., Hastings, D.F. and Ting-Beall, H.P. (1989) J. Microsc. 154 (P41), 71–82.
[17] Jørgensen, P.L. (1974) Methods Enzymol. 32, 277–290.
[18] Freytag, J.W. and Reynolds, J.A. (1981) Biochemistry 20, 7211–7214.
[19] Hastings, D.F., Reynolds, J.A. and Tanford, C. (1986) Biochim. Biophys. Acta 860, 566–569.
[20] Ball, W.J. (1984) Biochemistry 23, 2275–2281.
[21] Stanworth, D.R. and Turner, M.W. (1978) in: Handbook of Experimental Immunology, (Weir, D.M. ed) Blackwell Scientific/ Alden Press, Oxford, UK, pp.6.1–6.36.
[22] Frank, J., Shimkin, B. and Dowse, H. (1981) Ultramicroscopy 6, 343–358.
[23] Frank, J., Verschoor, A. and Boublik, M. (1981) Science 214, 1353–1355.
[24] Taylor, K.A., Dux, L. and Martonosi, A. (1986) J. Mol. Biol. 187, 417–427.
[25] Mohraz, M., Simpson, M.V. and Smith, P.R. (1987) J. Cell Biol. 105, 1–8.
[26] Castillani, L. and Hardwicke, P.M.D. (1983) J. Cell Biol. 97, 557–561.
[27] Buhle, E.L., Knox, B.E., Serpersu, E. and Aebi, U. (1983) J. Ultrastruc. Res. 85, 186–203.
[28] Dux, L., Taylor, K.A., Ting-Beall, H.P. and Martonosi, A. (1985) J. Biol. Chem. 260, 11730–11743.
[29] Castillani, L., Hardwicke, P.M.D. and Vibert, P. (1985) J. Mol. Biol. 185, 579–594.
[30] Jørgensen, P.L. and Collins, J.H. (1986) Biochim. Biophys. Acta 860, 570–576.
[31] Misra, M., Beall, H.C., Taylor, K.A. and Ting-Beall, H.P. (1988) Proc. 46th Annual Meeting Electron Microsc. Society of America, (Bailey, G.W. ed.) San Francisco Press, San Francisco, CA, pp.396–397.